XIX International Conference on Water Resources
CMWR 2012
University of Illinois at Urbana-Champaign
June 17-22, 2012

MODELING DENSITY-COUPLED STOKES FLOW AND MASS TRANSPORT THROUGH FRACTURES

Ali Zidane[1,2], Anis Younes [1], Peter Huggenberger[2], Eric Zechner[2]

[1] Laboratoire d'Hydrologie de Geochimie de Strasbourg, University of Strasbourg, CNRS, UMR 7517
[2] Department of Environmental Sciences, University of Basel, Institute of Geology, Switzerland

Keywords: variable density flow, Stokes flow, nonconforming finite elements, discontinuous finite elements, MPFA, analytical solution.

Summary In this work, a numerical model is developed for modelling coupled Stokes flow and mass transport in the case of large density variations. The Stokes flow equations are solved using the Crouzeix-Raviart (CR) approximation. For the transport equation, the Discontinuous Galerkin (DG) method is used for the discretization of the advection equation and combined with the symmetric Multi-Point Flux Approximation (MPFA) method for the discretization of the diffusion equation. A semi-analytical solution, obtained by expanding the salt concentration and the stream function in double Fourier series, is developed for a synthetic problem of salt water intrusion in a fracture and used for the validation of the numerical model.

1. INTRODUCTION

Fluid flow and transport trough fractures are important in environmental and petroleum engineering [1]. In this paper, we develop an accurate numerical model to simulate transport of salt water through cavities or fractures. In this case, the flow equations and the solute transport equations are coupled by the state equations linking density variations to mass fraction. In this work, the flow through cavities is considered steady and laminar and the inertial forces in the flow field are assumed to be negligibly small compared with the viscous and pressure forces. Therefore, the free-flow is governed by the Stokes equation [2, 3, 4, 5, 6, 7, and 8]. Different methods can be used for the discretization of the Stokes equation [9]. We use in this work the Crouzeix-Raviart (CR) approximation based on the nonconforming piecewise linear finite elements for the velocity and the piecewise constant finite elements for the pressure. For the transport equation, the Discontinuous Galerkin (DG) method is used to discretize the advection equation and combined with the symmetric Multipoint Flux Approximation (MPFA) method for the discretization of the diffusion equation [10]. The DG method allows to obtain a robust and accurate numerical scheme for problems involving sharp fronts [11]. On the other hand, the MPFA method is locally conservative and handles general irregular grids [12, 13, 14]. The MPFA and the DG discretization can be gathered into one system matrix without operator splitting [10]. Flow and transport equations are solved sequentially using a non iterative scheme with proper time management based on local truncation error control as in [15]. To validate the numerical code, we develop a semi-analytical solution for a synthetic problem of saltwater intrusion trough a cavity. This problem is obtained by replacing the confined aquifer (flow governed by Darcy flow) in the well known Henry [16] saltwater intrusion problem by a cavity (flow governed by Stokes free-flow). As with the standard Henry problem [16], we develop a semi-analytical solution by expanding the concentration and the stream function in a double set of Fourier series.

2. MATHEMATICAL MODELS

Single-phase steady incompressible flow through a fracture is governed by the Navier-Stokes equation:

$$\rho(\boldsymbol{u}.\nabla)\boldsymbol{u} + \nabla p - \mu\nabla^2\boldsymbol{u} = \rho\boldsymbol{g} \tag{1}$$

and the continuity equation:

$$\nabla.\boldsymbol{u} = 0 \tag{2}$$

where ρ is the fluid density, $\boldsymbol{u}$ is the velocity vector, p is the pressure, $\boldsymbol{g}$ is gravity, and μ is the dynamic viscosity.

We assume that the flow through the fracture is sufficiently slow to consider the inertial forces in the flow field (the first nonlinear term in equation(1)) negligibly small compared with the viscous and pressure forces. Therefore, in this case, the free-flow is governed by the following Stokes equations [17, 18, 19]:

$$\nabla p - \mu\nabla^2\boldsymbol{u} = \rho\boldsymbol{g} \tag{3}$$

$$\nabla.\boldsymbol{u} = 0 \tag{4}$$

In this work, three kinds of boundary conditions are used with this system:

- The velocity $\boldsymbol{u}$ is prescribed on the boundary;
- Free outflow boundary condition $\mu(\nabla\boldsymbol{u})\boldsymbol{\eta} - p\boldsymbol{\eta} = 0$ with $\boldsymbol{\eta}$ the outward normal vector to the boundary;
- The pressure p is prescribed at the boundary. Note that in this case, we set also the velocity components in the tangential direction to zero on the same boundary as used in [20, 21, 22, 23, 24]. This condition is named Normal flow/Pressure or straight-out boundary condition.

Solute transport in the free-flow region can be described by the following convection-diffusion equation:

$$\frac{\partial C}{\partial t} + \boldsymbol{u}.\nabla C = D\nabla^2 C \tag{5}$$

where C is the solute mass fraction and D is the molecular diffusion coefficient.

Flow and transport equations are coupled by the linear state equation linking density to mass fraction:

$$\rho = \rho_0 + (\rho_1 - \rho_0)C \tag{6}$$

with ρ_1 the density of the injected fluid and ρ_0 the freshwater density.

The boundary conditions for the transport equation are of Dirichlet type (C is fixed) or a convective boundary type ($\partial C/\partial\boldsymbol{\eta} = 0$ where $\boldsymbol{\eta}$ is the direction normal to the boundary).

3. STOKES FLOW DISCRETIZATION

The system (3)-(4) cannot be discretized with the same order for pressure and velocity approximations due to stability conditions. Otherwise some sort of stabilization is added to the mixed formulation [25]. To avoid these difficulties, we use the non-conforming Crouzeix-Raviart (CR) elements for the velocity approximation in combination with constant pressure per element, since they satisfy the Babuska-Brezzi condition [26, 27, 28]. This condition is central for ensuring that the final linear system to solve is non-singular [9]. Moreover, the non-conforming Crouzeix-Raviart (CR) element has local mass conservation properties [29] and leads to a relatively small number of unknowns due to the low-order shape functions. The

CR element is used in many problems such as the Darcy-Stokes problem [30], the Stokes problem [31] and the elasticity problem [32, 33]. The CR element gives a simple stable optimal order approximation of the Stokes equations [34]. In the following, we recall the main stages for the discretization of the Stokes equation with the CR triangular element.

With the non-conforming finite element method, the degrees of freedom for the velocity vector $\boldsymbol{u}$ are the two component (u_i, v_i) of $\boldsymbol{u}$ at the midedge i facing the node i. Inside the element E, we assume a linear variation of the velocity components (u_E, v_E)

$$u_E = u_i\varphi_i^E + u_j\varphi_j^E + u_k\varphi_k^E \quad , \quad v_E = v_i\varphi_i^E + v_j\varphi_j^E + v_k\varphi_k^E \tag{7}$$

For an interior edge, the linear interpolation function φ_i for the velocity is nonzero only on the two adjacent elements E and E', where $|E|$ is the area of the element E, x_i and z_i are the coordinates of the vertex i of E. The interpolation function φ_i^E equals 1 on the midedge i and zero on the midedges j and k of E.

The variational formulation of the Stokes equation (3) using the test function φ_i over the domain Ω writes:

$$\int_\Omega \nabla.\left(\mu\nabla\boldsymbol{u} - p\boldsymbol{I}\right)\varphi_i = \int_\Omega \rho g \nabla z \varphi_i \tag{8}$$

where $\nabla\boldsymbol{u}$ is the gradient of the velocity vector $\boldsymbol{u}$ and $\boldsymbol{I}$ the 2×2 identity matrix.

Using Green's formula,

$$\int_{\partial\Omega} \varphi_i \left(\mu\nabla\boldsymbol{u} - p\boldsymbol{I}\right)\boldsymbol{\eta}_{\partial\Omega} - \int_\Omega \nabla.\left(\mu\nabla\boldsymbol{u} - p\boldsymbol{I}\right)\varphi_i = \int_\Omega \rho g \nabla z \varphi_i \tag{9}$$

The first integral contains boundary conditions. It vanishes in case of free-flow boundary or in case of an interior edge i. In this last case, equation (9) becomes

$$-\int_E \nabla.\left(\mu\nabla\boldsymbol{u}_E - p_E\boldsymbol{I}\right)\varphi_i^E - \int_{E'} \nabla.\left(\mu\nabla\boldsymbol{u}_{E'} - p_{E'}\boldsymbol{I}\right)\varphi_i^{E'} = \int_E \rho g \nabla z \varphi_i^E + \int_{E'} \rho g \nabla z \varphi_i^{E'} \tag{10}$$

Using (7) and (8), we obtain

$$-\int_E \nabla.\left(\mu\nabla\boldsymbol{u}_E - p_E\boldsymbol{I}\right)\varphi_i^E = \begin{pmatrix}\Delta z^i \\ \Delta x^i\end{pmatrix} P_E - \frac{\mu}{|E|}\begin{pmatrix}\sum_{j=1}^{3}\left(\Delta x^i\Delta x^j + \Delta z^i\Delta z^j\right)u_j \\ \sum_{j=1}^{3}\left(\Delta x^i\Delta x^j + \Delta z^i\Delta z^j\right)v_j\end{pmatrix} \tag{11}$$

and

$$\int_E \rho g \nabla z \varphi_i^E = \rho_E g\left(\overline{z}_i - z_E\right)\begin{pmatrix}\Delta z^i \\ \Delta x^i\end{pmatrix} \tag{12}$$

where $\Delta x^i = x_j - x_k$ and $\Delta z^i = z_k - z_j$, z_E and $\overline{z}_i$ are respectively the z-coordinate of the centre of E and of the midpoint of edge i, ρ_E and p_E are respectively the mean density and pressure over E.

The finite volume formulation of the continuity equation (4) over the element E writes:

$$\int_E \nabla.\boldsymbol{u} = 0 \tag{13}$$

using (7), it becomes

$$\sum_{j=1}^{3}\left(\Delta z^{j}u_{j}+\Delta x^{j}v_{j}\right)=0 \tag{14}$$

4. TRANSPORT DISCRETIZATION

For the transport equation, standard numerical methods, such as standard finite elements or finite volumes, are known to generate solution with numerical diffusion and/or non-physical oscillations when advection is dominant. These problems can be avoided with DG [35]. Indeed, DG leads to a high-resolution scheme for advection that has been proven to be clearly superior to the already existing finite element methods [36].
In this work, the explicit DG method, where fluxes are upwinded using a Riemann solver is used to solve the advection equation and combined with the symmetric Multipoint Flux Approximation (MPFA) method for the diffusion equation.
The transport equation (5) is written in the following mixed form

$$\begin{cases}\dfrac{\partial C}{\partial t}+\boldsymbol{u}.\nabla C+\nabla.\left(\boldsymbol{u}_{D}\right)=0\\ \boldsymbol{u}_{D}=-D\nabla C\end{cases} \tag{15}$$

The dispersive flux $\boldsymbol{u}_D$ is assumed to vary linearly inside the element E, therefore,

$$\nabla.\boldsymbol{u}_{D}=\frac{1}{|E|}\sum_{i}Q_{D,\partial Ei}^{E} \tag{16}$$

where $Q_{D,\partial Ei}^{E}=\int_{\partial Ei}\boldsymbol{u}_{D}.\boldsymbol{\eta}_{\partial Ei}$ is the dispersive flux across the edge ∂Ei of E.

We use the $P1$ DG method where the approximate solution $C_h(\boldsymbol{x},t)$ is expressed with linear basis functions ϕ_i^E on each element E as follows:

$$C_{h}\left(\boldsymbol{x},t\right)|_{E}=\sum_{i=1}^{3}C_{i}^{E}\left(t\right)\phi_{i}^{E}\left(\boldsymbol{x}\right) \tag{17}$$

where $C_i^E(t)$ are the three unknown coefficients corresponding to the degrees of freedom which are the average value of the mass fraction defined at the triangle centroid $\left(\overline{x}_E,\overline{z}_E\right)$ and its deviations in each space direction [37] with the corresponding interpolation functions:

$$\phi_{1}^{E}\left(x,z\right)=1,\quad \phi_{2}^{E}\left(x,z\right)=x-\overline{x}_{E},\ \phi_{3}^{E}\left(x,z\right)=z-\overline{z}_{E}. \tag{18}$$

The variational formulation of (15) over the element E using ϕ_i^E as test functions leads to (see [10] for details),

$$\left[A\right]\begin{pmatrix}\dfrac{dC_{1}^{E}}{dt}\\ \dfrac{dC_{2}^{E}}{dt}\\ \dfrac{dC_{3}^{E}}{dt}\end{pmatrix}=\left[B\right]\begin{bmatrix}C_{1}^{E}\\ C_{2}^{E}\\ C_{3}^{E}\end{bmatrix}-\left[M^{0}\right]\begin{bmatrix}C_{1}^{E}\\ C_{2}^{E}\\ C_{3}^{E}\end{bmatrix}-\sum_{\ell=1}^{3}\left[M^{\ell}\right]\begin{bmatrix}C_{1}^{E\ell}\\ C_{2}^{E\ell}\\ C_{3}^{E\ell}\end{bmatrix}+\begin{bmatrix}\sum_{\partial Ej}Q_{D,j}^{E}\\ 0\\ 0\end{bmatrix} \tag{19}$$

with,

$$A_{i,j} = \int_E \phi_j^E \phi_i^E \qquad B_{i,j} = \int_E \phi_j^E \, \boldsymbol{u}.\nabla \phi_i^E$$

$$M_{i,j}^0 = \sum_{\ell=1}^{N_E} \lambda_{\partial E\ell}^E \frac{Q_{\partial E\ell}^E}{|\partial E\ell|} \int_{\partial E\ell} \phi_i^E \, \phi_j^E , \qquad M_{i,j}^\ell = \left(1-\lambda_{\partial E\ell}^E\right) \frac{Q_{\partial E\ell}^E}{|\partial E\ell|} \int_{\partial E\ell} \phi_i^E \, \phi_j^{E\ell} \qquad (\ell = 1,..,3)$$

where Ej is the adjacent element to E such that ∂Ej is the common edge of E and Ej and $Q_{\partial E\ell}^E = \int_{\partial E\ell} \boldsymbol{u}.\boldsymbol{\eta}_{\partial Ej}$ the water flux across ∂Ej. The upwind parameter $\lambda_{\partial E\ell}^E$ is defined by

$$\lambda_{\partial Ej}^E = \begin{cases} 1 & if \quad \boldsymbol{u}.\boldsymbol{\eta}_{\partial Ej} \geq 0 \\ 0 & if \quad \boldsymbol{u}.\boldsymbol{\eta}_{\partial Ej} < 0 \end{cases} \tag{20}$$

5. VALIDATION OF THE DENSITY-COUPLED FLOW TRANSPORT PROBLEM

5.1 The semi-analytical solution of saltwater intrusion trough a cavity

To validate the numerical code, a semi-analytical solution is developed for a synthetic problem of saltwater intrusion trough a cavity. We consider an idealized rectangular cavity in which freshwater enters with a constant flux rate Q from the left boundary. A hydrostatic pressure is prescribed along the right boundary where the concentration is fixed to salt-water concentration. The top and the bottom of the domain are impermeable boundaries. The saltwater intrudes from the right until an equilibrium with the injected freshwater is reached. The Stokes equations (3)-(4) are written in the following form:

$$\begin{cases} -\dfrac{\partial P}{\partial x} + \mu\left(\dfrac{\partial^2 u}{\partial x^2} + \dfrac{\partial^2 u}{\partial z^2}\right) = 0 \\ -\dfrac{\partial P}{\partial z} + \mu\left(\dfrac{\partial^2 v}{\partial x^2} + \dfrac{\partial^2 v}{\partial z^2}\right) = f \\ \dfrac{\partial u}{\partial x} + \dfrac{\partial v}{\partial z} = 0 \end{cases} \tag{21}$$

where the body forces f can be written using (6) in the following form,

$$f = \left[\rho_0 + (\rho_1 - \rho_0)C\right] g \tag{22}$$

The last equation in (21) implies the existence of a stream function ϕ, such as:

$$u = \frac{\partial \phi}{\partial z} \text{ and } v = -\frac{\partial \phi}{\partial x} \tag{23}$$

Inserting (23) into (21) leads to:

$$\mu\left[\frac{\partial^4 \phi}{\partial x^4} + 2\frac{\partial^4 \phi}{\partial x^2 \partial z^2} + \frac{\partial^4 \phi}{\partial z^4}\right] = -(\rho_1 - \rho_0) g \frac{\partial C}{\partial z} \tag{24}$$

As in [16, 38], we define the following new variables:

$$x' = x/d \,,\; z' = z/d \,,\; u' = u\,d/Q \,,\; v' = v\,d/Q \,,\; u' = \partial\psi'/\partial z' \,,\; v' = -\partial\psi'/\partial x' \,,\; \psi = \psi' - z' \tag{25}$$

where x' and z' are non-dimensional coordinates, u' and v' are the non-dimensional velocities and ψ' the non dimensional stream function.

Using (25), eq (24) leads to:

$$a\left(\frac{\partial^4\psi}{\partial x^4}+2\frac{\partial^4\psi}{\partial x^2\partial z^2}+\frac{\partial^4\psi}{\partial z^4}\right)=-\left(\frac{\partial C}{\partial x}+\frac{1}{\xi}\right) \tag{26}$$

with $a=\frac{\mu Q}{(\rho_1-\rho_0)gd^3}$ and $\xi=\frac{L}{d}$ the aspect ratio of the domain, where L is the length and d is the depth of the domain.

Similarly, the change of variables applied to the mass transport equation (5) (see [16, 38] for details) leads to:

$$b\left(\frac{\partial^2 C}{\partial x^2}+\frac{\partial^2 C}{\partial z^2}\right)=\frac{\partial\psi}{\partial z}\frac{\partial C}{\partial x}-\frac{\partial\psi}{\partial x}\frac{\partial C}{\partial z}+\frac{1}{\xi}\frac{\partial\psi}{\partial z}+\frac{\partial C}{\partial x}+\frac{1}{\xi} \tag{27}$$

with $b=\frac{D}{Q}$ and C is now the non-dimensional concentration.

The stream function and the concentration are represented by double Fourier series of the form:

$$\psi=\sum_{m=1}^{\infty}\sum_{n=0}^{\infty}A_{m,n}\sin(m\pi z)\cos(n\pi\frac{x}{\xi}) \tag{28}$$

$$C=\sum_{r=0}^{\infty}\sum_{s=1}^{\infty}B_{r,s}\cos(r\pi z)\sin(s\pi\frac{x}{\xi}) \tag{29}$$

Substituting these relations into equations (26) and (27), multiplying equation (26) by $4\sin(g\pi z)\cos(h\pi\frac{x}{\xi})$ and equation (27) by $4\cos(g\pi z)\sin(h\pi\frac{x}{\xi})$, and integrating over the rectangular domain gives an infinite set of algebraic equations for $A_{g,h}$ and $B_{g,h}$ namely,

$$\varepsilon_2 a\pi^4 A_{g,h}(g^2+\frac{h^2}{\xi^2})^2\xi=\sum_{r=0}^{\infty}B_{r,h}hN(g,r)+\frac{4}{\pi}W(g,h) \tag{30}$$

$$\varepsilon_1 b\pi^2 B_{g,h}(g^2+\frac{h^2}{\xi^2})\xi=\sum_{n=0}^{\infty}A_{g,n}gN(h,n)+\varepsilon_1\sum_{s=1}^{\infty}B_{g,s}SN(h,s)+Quad+\frac{4}{\pi}W(h,g) \tag{31}$$

Details about the parameters $\varepsilon_1,\varepsilon_2,N,W,Quad$, can be found in [16].

5.2 Validation of the numerical model

We consider a synthetic example where the domain is discretized with a regular triangular mesh of 3200 elements. The flux at the left (inland) boundary is $Q=0.92\,m^2s^{-1}$ and the diffusion coefficient is set to $D=0.046\,m^2s^{-1}$, the densities of freshwater (at the left boundary) and saltwater (at the right boundary) are respectively $\rho_0=1000\,kg\,m^{-3}$ and $\rho_1=1015\,kg\,m^{-3}$. To avoid very small values of the parameter a for which, we cannot obtain a converged semi-analytical solution, the viscosity is set to $\mu=1$ Pa s in this synthetic problem. The corresponding parameters for the analytical solution are $a=\frac{\mu Q}{(\rho_1-\rho_0)gd^3}=0.006$ and $b=\frac{D}{Q}=0.05$.

To reduce these oscillations, the semi analytical solution is performed with a new truncation using 424 coefficients of the Fourier series with 214 terms $\left(A_{1..7,0..30}\right)$ for the expansion of the

stream function and 210 terms $\left(B_{0..6,1..30}\right)$ for the expansion of the concentration. A good agreement is observed between the semi-analytical and numerical results in this case (Figure 1). These results demonstrate the validity of the numerical model. The developed analytical solution can be used for the validation of other numerical codes.

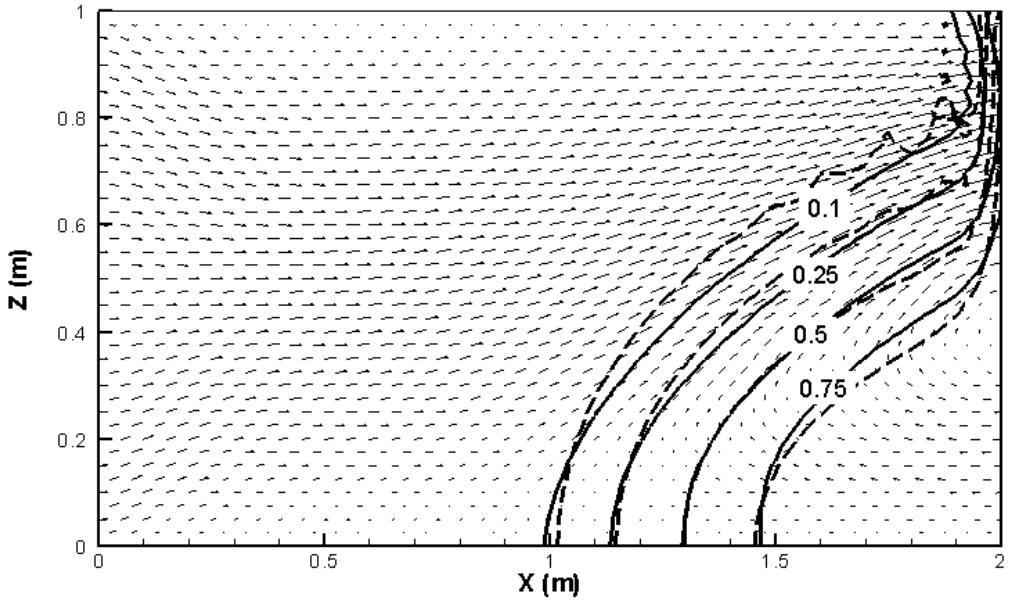

Figure 1: Semi-analytical (dashed lines) and numerical isochlors (solid lines) and numerical velocity field for the saltwater intrusion problem through a cavity. The semi-analytical solution is calculated using a truncation based on 424 coefficients for the double Fourier series.

6. CONCLUSION

In this manuscript, we developed an efficient numerical model to simulate transport of saltwater through cavities or fractures. In this case, the flow equations and the solute transport equations are coupled by the state equations linking density variations to mass fraction. The model is developed for a general triangular mesh and uses the CR finite elements for the flow discretization, the DG method for advection and the symmetric MPFA method for diffusion.
The developed model is used for the simulation of a synthetic problem of saltwater intrusion trough a cavity. This problem is adapted from the saltwater intrusion problem of Henry [16], by replacing the confined aquifer by a cavity. The semi-analytical solution is developed for this problem by expanding the stream function and the concentration in double Fourier series. The algebraic equations are then solved using the Levenberg-Marquardt algorithm [39]. The analytical solution is developed for a new truncation (424 terms). With the new truncation, the unphysical oscillations are reduced for the semi-analytical solution and a good agreement is observed with the numerical solution.

References

[1]M. Bayani Cardenas, Donald T. Slottke, Richard A. Ketcham, John M. Sharp Jr., Navier-Stokes flow and transport simulations using real fractures shows heavy tailing due to eddies, *Geophysical Research Letters*, Vol.34, L14404, doi:10.1029/2007GL030545, 2007

[2]G. Beavers and D. Joseph, Boundary conditions at a naturally permeable wall, *J. Fluid Mech.*, (1967) 30:197.

[3]P. Saffman. On the boundary condition at the surface of a porous medium, *Studies Appl. Math*. (1971) 50:93.

[4]E. Sanchez-Palencia, Non-Homogeneous Media and Vibration Theory, volume 127 of *Lecture Notes in Physics* (1980), Spring-Verlag, Berlin.

[5]M. Kaviany, Principles of Heat Transfer in Porous Media, *Mechanical Engineering Series* (1999), Springer-Verlag, New York.

[6]W. Jäger and A. Mikelić, On the interface boundary condition of Beavers, Joseph, and Saffman. *SIAM J. Appl. Math* (2000). 60:1111.

[7]W. Jäger and A. Mikelić, Asymptotic analysis of the laminar viscous flow over a porous bed. *SIAM J. Sci. Comput.*(2001a) 22:2006.

[8]T. Arbogast and H.L. Lehr, Homogenization of a Darcy-Stokes system modeling vuggy porous media. *Comput. Geosci.*(2006), 10:291.

[9]H.P. Langtangen, K. Mardal, R. Winther, Numerical methods for incompressible viscous flow. *Adv. Water Res*. 25 (2002) 1125-1146.

[10]A. Younes, P. Ackerer, Solving the advection-dispersion equation with Discontinuous Galerkin and Multipoint Flux Approximation methods on unstructured meshes. *Int. J Numer Methods in Fluids*. 2008; DOI: 10.1002/fld.1783.

[11]T. Shuangzhang, A. Shahrouz, A slope limiting procedure in Discontinuous Galerkin finite element method for gasdynamics applications. *Int. J Numer Analy Modell* 2005;2:163-178.

[12]I. Aavatsmark, An introduction to multipoint flux approximations for quadrilateral grids. *Comput Geosci* (2002);6:404–432.

[13]I. Aavatsmark , T. Barkve, Ø. Bøe, T. Mannseth, Discretization on non-orthogonal, quadrilateral grids for inhomogeneous, anisotropic media. *J Comput Phys* (1996);127:2–14.

[14]MF. Wheeler, I. Yotov. A multipoint flux mixed finite element method. SIAM44 2006;5:2082-2106.

[15]A. Younes and P. Ackerer, Empirical versus time stepping with embedded error control for density-driven flow in porous media, *Water Resour. Res.*(2010), 46, W01504, doi:10.1029/2009WR008229

[16]H.R. Henry, Effects of dispersion on salt encroachment in coastal aquifers, in *Sea Water in Coastal Aquifers, U.S. Geol. Surv. Supply Pap.,* (1964),1613-C, 70 – 84.

[17]E. G. Flekkøy, T. Rage, U. Oxaal, and J. Feder, Hydrodynamic Irreversibility in Creeping Flow, *Phys. Rev*(1996), PACS numbers: 47.15.Gf, 02.70.Bf, 02.70.Lq, 47.60.+I, VOLUME 77, NUMBER 20

[18]J. Happel and H. Brenner, *Low Reynolds Number Hydrodynamics* (Prentice Hall Inc., Englewood Cliffs, NJ,1965).

[19]L. D. Landau and E. M. Lifshitz, *Fluid Mechanics* (Pergamon Press, New York, 1987), 2nd ed.

[20]C. Conca, F. Murat, O. Pironneau, The Stokes and Navier-Stokes equations with boundary conditions involving the pressure. *Jpn J. Math.* 20, 263-318 (1994)

[21]C. Conca, C. Parés, O. Pironneau, M. Thiriet, Navier-Stokes equations with imposed pressure and velocity fluxes. *Int. J. Numer. Methods Fluids* 20(4), 267-287 (1995)

[22]P.M. Gresho, R.L. Sani, On pressure boundary conditions for the incompressible Navier-Stokes equations. *Int. J. Numer. Methods Fluids* 7, 1111-1145 (1987)

[23]W. Jäger and A. Mikelić, On the roughness-induced effective boundary conditions for an incompressible viscous flow, *J. Differ. Equ*. 170, 96-122 (2001b)

[24]G. Lukaszewicz, On the Navier-Stokes equations in time dependent domains with boundary conditions involving the pressure. *J. Math. Sci*. Univ. Tokyo 4, 529-550 (1997)

[25]J. Li, Z. Chen, A new local stabilized nonconforming finite element method for the Stokes equations, *Computing* (2008), 82:157-170, doi 10.1007/s00607-008-0001-z

[26]F. Brezzi, M. Fortin, Mixed and hybrid finite element methods, Berlin: Springer 1991.

[27]V. Girault, PA. Raviart, Finite element methods for Navier-Stokes equations, Berlin: Springer 1986

[28]PM. Gresho, RL. Sani, Incompressible flow and the finite element method, New York: Wiley; 1998

[29]E. Bruman, P. Hansbo, A stabilized nonconforming finite element method for incompressible flow, *Comput. Methods App0 Mech. Eng.*, vol. 195, num. 23-24, p. 2881-99, (2004).

[30]E. Bruman, P. Hansbo, Stabilized Crouzeix-Raviart element for the Darcy-Stokes problem, *Numerical Methods for Partial Differential Equation,* 21(5), 986-997 (2005)

[31]M. Crouzeix, P. Raviart, Conforming and nonconforming finite element methods for solving the stationary Stokes equations. *RAIRO Sér. Rouge*, 7(3), 33-75 (1973)

[32]P. Hansbo, M.G. Larson, Discontinuous Galerkin and the Crouzeix-Raviart element: application to elasticity. *ESAIM: Math. Model. Numer. Anal.* 37(1), 63-72 (2003)

[33]P. Hansbo, M.G. Larson, Discontinuous Galerkin methods for incompressible and nearly incompressible elasticity by Nitshe's method. *Comput. Methods Appl. Mech. Engrg*, 191(17-18), 1895-1908 (2002)

[34]D.N. Arnold, On nonconforming linear-constant elements for some variants of the Stokes equations, presenta dal s.c. Franco Brezzi nella seduta del 24-6-93.

[35]P. Siegel, R. Mosé , P. Ackerer, J. Jaffre, Solution of the advection-diffusion equation using a combination of discontinuous and mixed finite elements. *Int J Numer Meth in Fluids* 1997; 24(6): 595-613.

[36]DN. Arnold, F. Brezzi, B. Cockburn,LD. Marini, Unified analysis of discontinuous Galerkin methods for elliptic problems. *SIAM J. Numer. Anal*. 2002;5:1749-1779.

[37]B. Cockburn, S. Hou, CW. Shu, TVB Runge Kutta local projection discontinuous Galerkin finite element method for conservative laws III: One dimensional systems, *J. Compu.t Phys.* 1989;84: 90-113.

[38]G. Segol, Classic Groundwater Simulations Proving and Improving Numerical Models, Prentice-Hall, Old Tappan, N. J. (1994)

[39]D.W. Marquardt, An algorithm for least-squares estimation of nonlinear inequalities, SIAM *J. Appl. Math*., (1963) ,11 , 431-441.